



## Detection principles of biological and chemical FET sensors



Matti Kaisti

University of Turku, Department of Future Technologies, FI-20014 Turun yliopisto, Finland

### ARTICLE INFO

#### Keywords:

Biosensor  
Chemical sensor  
FET  
ISFET  
Detection  
Electrochemistry

### ABSTRACT

The seminal importance of detecting ions and molecules for point-of-care tests has driven the search for more sensitive, specific, and robust sensors. Electronic detection holds promise for future miniaturized in-situ applications and can be integrated into existing electronic manufacturing processes and technology. The resulting small devices will be inherently well suited for multiplexed and parallel detection. In this review, different field-effect transistor (FET) structures and detection principles are discussed, including label-free and indirect detection mechanisms. The fundamental detection principle governing every potentiometric sensor is introduced, and different state-of-the-art FET sensor structures are reviewed. This is followed by an analysis of electrolyte interfaces and their influence on sensor operation. Finally, the fundamentals of different detection mechanisms are reviewed and some detection schemes are discussed. In the conclusion, current commercial efforts are briefly considered.

### 1. Introduction

Among various potentiometric techniques, sensing based on field-effect transistors (FETs) has attracted considerable attention because of its potential for miniaturization, parallel sensing, fast response time, and seamless integration with electronic manufacturing processes, such as complementary metal-oxide semiconductors (CMOS) [Chen \(2013\)](#); [Schoning and Poghossian \(2002\)](#); [Poghossian and Schöning \(2014\)](#). The concept of an ion-sensitive FET (ISFET) was introduced in the early 1970s and it was derived from a metal-oxide-semiconductor FET (MOSFET) [Bergveld \(2003\)](#). It was realized that a MOSFET with the metal gate removed and the underlying gate oxide inserted in an aqueous solution along with a reference electrode could be used detect ions. Given the importance of the hydrogen ion, most early research focused on its detection through experimental and modeling developments [Bergveld \(2003\)](#), whereas more recent efforts emphasize various gate-modification techniques towards the detection of biomolecular interactions [Schoning and Poghossian \(2002\)](#); [Poghossian and Schöning \(2014\)](#). Interestingly, the coated-wire electrode, analogous to the ISFET technology, was invented at the same time [Cattrall and Freiser \(1971\)](#). It was designed to simplify the conventional ion-selective electrode (ISE) that requires internal filling solutions in conjunction with an ion-selective membrane (ISM). The coated-wire arrangement consists of either a metal wire or a disk electrode directly coated with an ISM. This results in a much simpler, smaller, inexpensive, and robust sensor compared to the conventional ISE. The potential of the electrode is measured against a reference electrode

using a high-impedance voltmeter. There are no ohmic potential drops in the system because it operates (ideally) in zero-current condition. The measured potential is the sum of many interfacial potentials, but only the interfacial potential between the sample and the gate material varies depending on the target analyte activity [Hu et al. \(2016\)](#). This principle also applies to FET-based sensors. In fact, the input terminal of the voltmeter is simply a FET, and only the surrounding circuit and biasing are different compared to conventional potentiometric setup. Additionally the used electrodes are different, but the reason is mostly practical.

There are many different FET sensor structures and sensing materials. Along with different target analytes, it results in a myriad of different sensor system combinations. These systems share the same overall construction that is illustrated in [Fig. 1](#). The information obtained from the sample corresponds to either the concentration/activity of the target analyte or the presence/quantity of a biomolecule, which is transduced to an electrical signal via the field effect. Then, the signal can be amplified, processed, and displayed [Schoning and Poghossian \(2002\)](#) or sent to the cloud [Nemiroski et al. \(2014\)](#) depending on the application.

This review focuses on different transistor structures and on the interfacial behavior at the electrolyte-solid interface. I omit structures such as silicon nanowire (SiNW) FETs and graphene FETs because they are extensively covered elsewhere. For recent reviews beyond the scope of this work, the reader can refer to the following: broad and general electrochemical sensor reviews [Privett et al. \(2010\)](#); [Ronkainen et al. \(2010\)](#); [Perumal and Hashim \(2014\)](#), CMOS-based sensing [Arya et al.](#)

E-mail address: [mkaist@utu.fi](mailto:mkaist@utu.fi).

<http://dx.doi.org/10.1016/j.bios.2017.07.010>

Received 12 April 2017; Received in revised form 21 June 2017; Accepted 4 July 2017

Available online 05 July 2017

0956-5663/© 2017 The Author. Published by Elsevier B.V. This is an open access article under the CC BY-NC-ND license (<http://creativecommons.org/licenses/by-nc-nd/4.0/>).

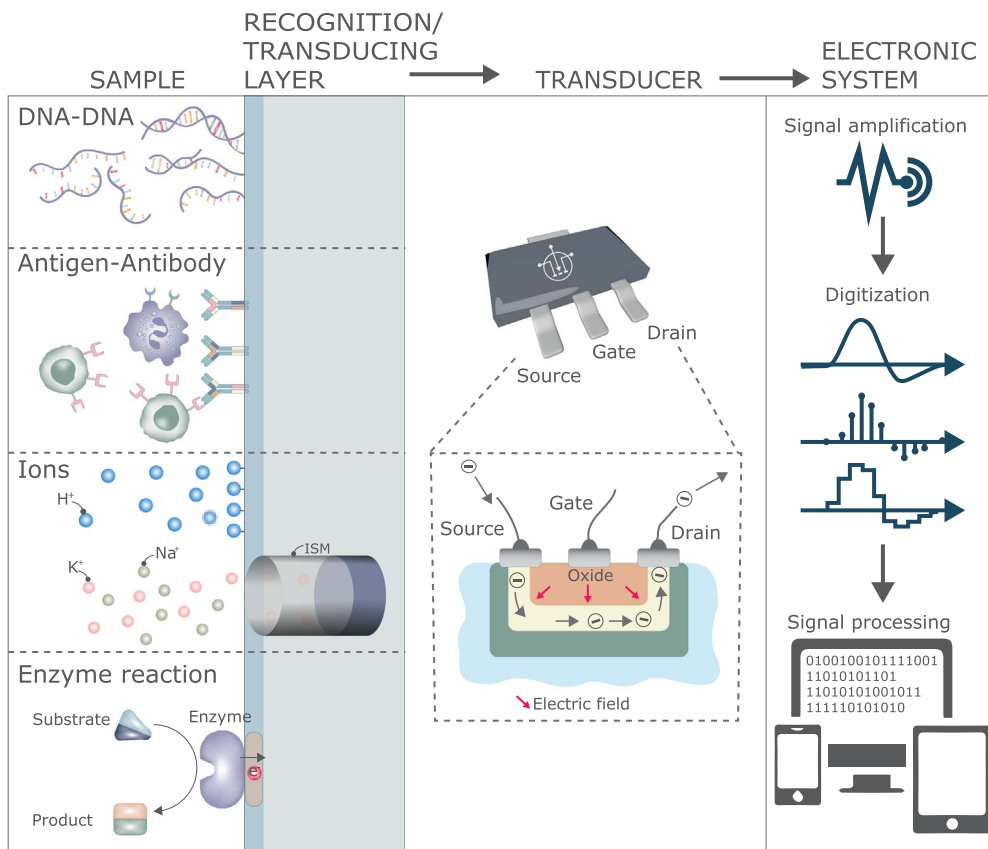


Fig. 1. Illustration of a biological and chemical FET sensor.

(2015); Lei et al. (2016), label-free detection Poghossian and Schöning (2014); Mehrabani et al. (2014), electrochemical immunosensors for point-of-care diagnostics Wan et al. (2013), nucleic acid diagnostics Ahmad and Hashsham (2012), wearable chemical sensors Matzeu et al. (2015); Bandodkar et al. (2016), lab-on-chip applications Lafleur et al. (2015), and SiNW biosensors Zhang and Lieber (2016).

1.1. Biological and chemical FET sensors

A simplified potential diagram of a generalized (bio)chemical sensor is shown in Fig. 2, which conveys the necessary information required to understand the basic detection principle. Shoorideh and Chui (2014). The observed responses originate from charge  $\sigma_0$  resting at the sensing surface. This charge sees capacitances on both of its sides with signal grounds that follow. The capacitance is presented as a parallel combination of the double-layer and sensor (i.e., FET) capacitances,  $C_{DL}$  and  $C_{FET}$ , respectively, where the latter comprises the gate oxide,  $C_{OX}$ , and depletion,  $C_b$ , capacitances. The potential change at the sensing surface can be approximated by

$$\psi_0 = \frac{\Delta\sigma_0}{C_{DL} + C_{FET}} \tag{1}$$

Depending on the transistor biasing, either of these capacitances can dominate. In weak inversion,  $C_b$  will clearly be smaller and determine the overall sensor capacitance, in contrast to strong inversion, where  $C_b$  can be omitted and  $C_{OX}$  is relevant Streetman and Banerjee (2006). In either case, these capacitances are usually clearly smaller than the double-layer capacitance. Thus, the double layer strongly couples the potentials and, in many cases, it can be omitted from Eq. (1). Hence, we can conclude that in these cases the transistor capacitance has a negligible effect on the sensitivity at the sensing interface.

An attempt has been made to dissect the biosensor into indepen-

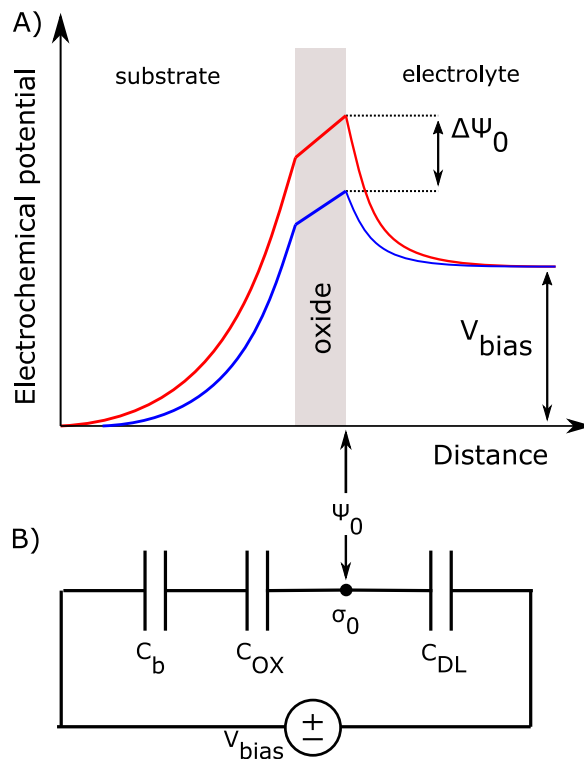


Fig. 2. A) Potential over a simplified model of electrochemical cell with an oxide as the interfacial material. The charge binding in the surface creates a potential shift, denoted by  $\Delta\psi_0$ , at the interface. The effect of Debye screening is observed in both the electrolyte solutions and semiconductor regions. B) Equivalent circuit model of the sensor where  $C_{DL}$ ,  $C_{OX}$ ,  $C_b$  are the double-layer, gate oxide, and depletion capacitances, respectively. The interfacial charge,  $\sigma_0$ , is shared by capacitors on both sides. Adapted from Shoorideh and Chui (2014).

dent parts for better understanding of the underlying physics [Shoorideh and Chui \(2014, 2012\)](#). First, the charge at the sensing surface alters the oxide electric field, changing the potential at the outer surface of the electrode. Second, this potential shift subsequently alters the semiconductor drain current. The latter is merely the transconductance effect of a FET. A nanoscale sensor shows no advantage in this effect over more conventional FET sensors, and therefore it has been concluded that the nanoscale advantage lies in the first part [Shoorideh and Chui \(2014\)](#). This effect is determined by the electrode–electrolyte interfacial properties, where the counter-ion screening is the most prominent factor.

The structure in this review follows a similar analysis of independent effects. In addition, different FET sensor electrical structures followed by interfacial properties are reviewed.

## 2. FET sensor structures

This section discusses various FET sensor structures. Several publications considered are based on ISFETs and pH detection, but the structures are applicable beyond pH sensing and state-of-art including biosensing is reviewed.

### 2.1. ISFETs in unmodified CMOS

A significant step forward in the development of ISFET sensors was the use of unmodified CMOS processes to create pH-sensitive arrays [Toumazou et al. \(2013\)](#); [Bausells et al. \(1999\)](#); [Milgrew et al. \(2005\)](#). Modern CMOS processes are highly robust and optimized, and they allow significant scalability and low-power operation, making them an ideal technology for handheld sensing devices. The unmodified ISFET variant is created by extending the metal gate up to the top layer of the chip. On top of this gate, a passivation layer is deposited. This approach allows unmodified CMOS processes to use this layer for pH sensing. This structure is shown in [Fig. 3-B](#).

The glass passivation commonly used in the CMOS process is a double layer of  $\text{SiO}_2\text{-Si}_3\text{N}_4$ . This layer creates an additional series capacitor compared to the original design shown in [Fig. 3-A](#), thus forming a capacitive division at the input that limits the sensitivity [Hu and Georgiou \(2014\)](#). In addition, the layer creates a poorly defined sensing capacitance as it extends over the entire chip, and it is usually much thicker than it would be using a freely chosen design. The effect of the sensing element geometry (e.g., size and shape) as well as the impact of technology scaling have been analyzed on the sensor performance [Sohbati and Toumazou \(2015\)](#); [Miscourides and Georgiou \(2015\)](#) and were found to affect parasitic capacitance coupling. Furthermore, the use of the passivation layer for sensing creates threshold variations of several volts between individual sensors due to the trapped charge within the layer [Liu et al. \(2011\)](#). Despite the abovementioned drawbacks, the use of an unmodified CMOS process considerably improves the reliability and allows mass fabrication, even though the encapsulation of the bond wires and electrical part is still necessary before it can be applied to wet environments. The resulting device has been highly successful in applications based on pH measurements, such as real-time detection of amplified nucleic acid [Toumazou et al. \(2013\)](#) and next-generation genome sequencing [Rothberg et al. \(2011\)](#).

### 2.2. Floating-gate FET sensor

A floating-gate structure with an additional control gate has been demonstrated by various groups [Shen et al. \(2003\)](#); [Barbaro et al. \(2006a\)](#), (2006b); [Jayant et al. \(2013a\)](#), (2013b), (2015); [Zhang et al. \(2015a\)](#). These ion-sensitive FGFET devices have two gates, where one gate serves as a sensing gate and the other as a control gate, as shown in [Fig. 3-C](#). Electrically, both gates have an analogous operation and they are capacitively coupled to a common floating gate. Changes in potential at either of these gates modulate the floating gate potential. In chemical sensing, one gate is reserved for control and can be used for

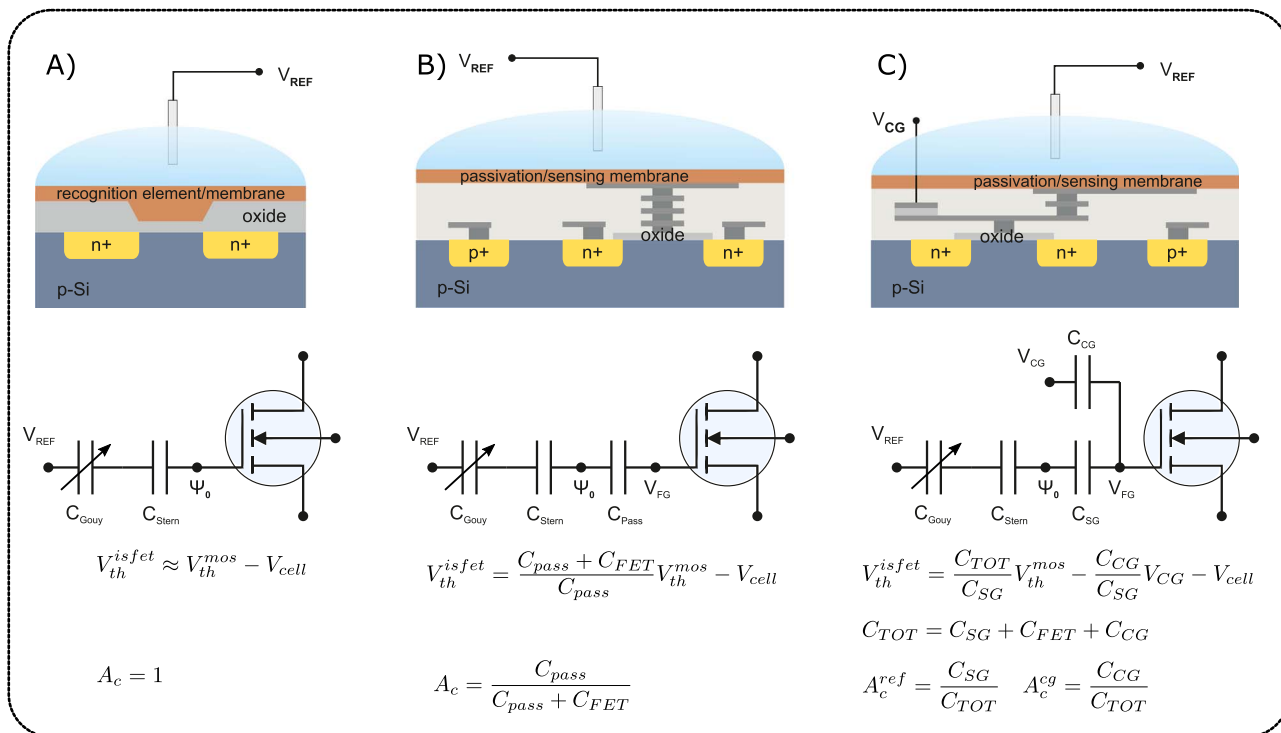


**Fig. 3.** Different FET sensor structures. A) Conventional structure with the gate metal removed and an optional recognition element/membrane deposited on top of the gate. Adapted from [Kaisti \(2017\)](#). B) Unmodified CMOS pH ISFET where a glass passivation layer is used as the sensing layer. Adapted from [Kalofonou and Toumazou \(2014\)](#). C) Control-gate assisted FET to tune the operation point and the charging of both the surface and the fluidic part. Adapted from [Kaisti et al. \(2015a\)](#). Constructions based on additional series capacitors at the input suffer from attenuated sensitivity due to the capacitive division. These are given as attenuation coefficients denoted by  $A_c$ .

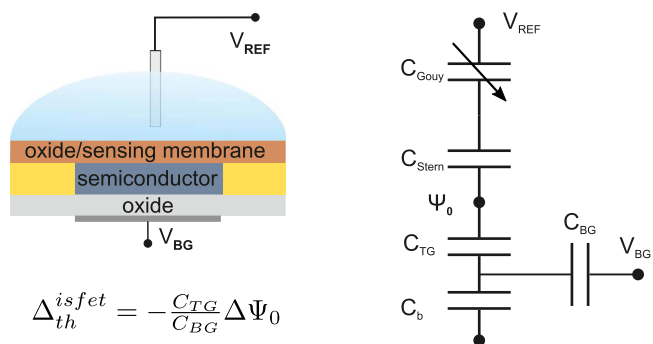


**Fig. 4.** DG-ISFET with its corresponding equivalent circuit. The increased pH slope, measured as back-gate threshold shifts, is due to the difference in capacitive coupling between the two gates. Information and figure derived from Spijkman et al. (2011a); Knopfmacher et al. (2010); Maddalena et al. (2008).

biasing, whereas the other serves as the sensing gate that is constructed to yield a response from the desired target.

Research on a charge-modulated FET to detect the intrinsic negative charge of the DNA molecule using a control gate has been presented Barbaro et al. (2006a), (2006b), (2012). The basic principle relies on the assumption that the charged DNA molecules induce a change in the threshold voltage at the floating gate without the presence of a reference electrode. In fact, several studies have achieved successful detection without using a reference electrode. However, this is either done in dry conditions Zhang et al. (2015a) or significant instabilities have been reported Guan et al. (2013), which most likely results from the fact that both the probe and electrolyte solution is in a floating potential.

More recent studies have shown that the surface charging can be programmed using control-gate-assisted modulation of the charge at the floating gate Jayant et al. (2013a), (2013b), (2015). This device was used for both pH and DNA sensing Jayant et al. (2013a), (2013b). The latter was achieved in three different readout modes including one without a reference electrode. In all the modes, the achievable surface potential changes were to some extent larger than those usually reported Poghossian et al. (2005); Poghossian and Schöning (2014). The reason for this is not fully understood, but it is speculated that the ability to alter the electric field of the sensing oxide causes a counterion descreening. A similar conclusion was reached by simulating a general silicon-on-insulator device Shoorideh and Chui (2012). Moreover, the detection was found to be most sensitive when the electric field near the analytes is zero. One possible solution is to bring charged groups to the vicinity of the insulator surface for optimizing the interfacial charge Vaknin et al. (2011). Another, perhaps more elegant solution using the structure under discussion, is to use electric-field modulation. This property has been termed as electrofluidic gating Jiang and Stein (2010) and considered theoretically feasible Kaisti et al. (2015a).

### 2.3. Extended-gate FET sensor

For general (bio)chemical sensing, the most straightforward FET structure resembling both conventional ISFETs and the coated wire is the extended-gate FET (EGFET) Kaisti et al. (2016); van der spiegel et al. (1983). A benefit of this compared to other FET structures stems from the separation of the wet and dry environments. In this structure, the sensing pad extends off chip, and only the off-chip sensing pad is immersed into the solution. Thus, the device fabrication is significantly simpler and allows convenient post-processing steps as its surface can be independently engineered from the transducer. However, the traces between the electronics and the sensing areas cannot be manufactured with printed circuit board technologies as compactly as with CMOS manufacturing processes although for many in-situ measurements the scalability is sufficient. Compared to coated-wire technologies, the

EGFET transduces the signal from a high- to a low-impedance environment physically significantly closer to the interface, avoiding the need for Faraday shielding Kaisti et al. (2016).

Recently, this seemingly simple structure has been used for different sensing concepts as follows. A pH sensing was demonstrated with off-the-shelf components Prodromakis et al. (2011a), (2011b); Kaisti et al. (2015b), and an electrical enzyme-linked immunosorbent assay (ELISA) was tested in cattle to detect specific BHV-1 antibodies produced in response to a viral infection Tarasov et al. (2016). The extended-gate structure has also been used to measure extracellular K<sup>+</sup> concentration with microfabricated sensing pads Odijk et al. (2015). An aptamer-probe-based extended-gate sensor has been used to monitor the tenofovir drug concentration with the aim to keep it within its therapeutic range Aliakbarinodehi et al. (2017). A handheld integrated device with a multipurpose extended-gate platform has also been presented Kaisti et al. (2016). In addition, extended-gate gold pads have been used for DNA detection Kamahori et al. (2008); Ishige et al. (2006) and as enzyme sensors for cholesterol detection Ishige et al. (2009).

### 2.4. Dual-gate FET sensor

The double-gate ISFET (DG-ISFET) has a similar structure to that of the FGFET sensor described in Section 2.2. It has been mainly studied for pH sensing with the aim to go beyond the Nernstian sensitivity and on a minor scale to DNA detection by utilizing thin-film transistors Spijkman et al. (2011a), (2011b); Jang and Cho (2014), SiNW FETs Knopfmacher et al. (2010), and CMOS technology Huang et al. (2015); Duarte-Guevara et al. (2014).

The DG-ISFET structure (see Fig. 4) employs an additional back gate yielding an increased slope in the sensor response. This is caused by the capacitive coupling between the usually thin top gate and thick bottom gate. It is important to realize that this is not a surface phenomenon. In fact, some studies reveal that despite the enhanced threshold shift (measured from the back gate), the sensor provides clearly sub-Nernstian slopes at the liquid gate Spijkman et al. (2011a). These measurements are done by sweeping the back gate and recording the threshold shifts produced by a chemical recognition at the top gate. This simply means that a potential shift at the top gate needs to be compensated by the shifts from the back gate, such that the current returns to the level prior to the chemical reaction. Thus, if the back gate is weakly coupled, it requires a large potential for compensation.

Recently, the use of an ultra-thin body improved the sensitivity of the DG-ISFET under study, and the drift was suppressed owing to fewer leakage components Jang and Cho (2014). DG-ISFETs implemented in CMOS have shown improved pH sensitivity and signal-to-noise ratio (SNR), as well as reduced drift and hysteresis Huang et al. (2015). However, the sensor requires postprocessing, where an isolated sensing gate is created by opening the back of the transistor and depositing a high-k dielectric. The following quantitative improvements are reported for the dual-gate operation: 155×SNR improvement (estimated from the power spectral density), 53×drift rate, 3.7×hysteresis reduction, and 7.5×sensitivity improvement Huang et al. (2015).

## 3. Solid–electrolyte interfaces

Although work has been performed on noise processes and effect of miniaturization in (bio)chemical sensors, these studies are still scarce and noncoherent due to the sensor complexity that includes various electrical structures, interfacial materials, functionalizations and sample-solution compositions. Regardless, this section attempts to cover the fundamental properties and debated issues concerning interfacial stability, scaling laws together with sensitivity and detection limit improvement. Emphasis is given to the actual detection rather than on effects of pretreatment processes.

### 3.1. Stability of interfaces

ISFETs are commonly fabricated using an oxide as the sensing layer. These sensors have a monotonic drift that has been attributed to buried sites in the oxide layer [Jamasp et al. \(1998\)](#). This drift is usually strongest when the sensor is exposed to a solution, and the potential response starts to stabilize afterwards. The buried sites are slowly protonated/deprotonated due to hydrogen ions diffusing into the oxide, leading to the drift. Compensation techniques for the drift include correction algorithms [Hammond et al. \(2005\)](#), direct hardware front-end solutions [Hu and Georgiou \(2014\)](#), and potential switching of the reference electrode [Welch et al. \(2013\)](#).

Another effect on ISFETs is the  $1/f$  noise, which manifests as a drift caused by random fluctuations over long time intervals. ISFETs manufactured through unmodified CMOS processes present significantly more  $1/f$  noise than the corresponding MOSFET on the same die. On contrary, the  $1/f$  noise in ISFETs have been found to be dominated by the FET parts itself [Jakobson and Nemirovsky \(1999\)](#) and that the noise dependence to drain current is similar to MOSFET and pH invariant. The latter, however, used a commercial pH meter with probably much thinner sensing layer which is expected decrease  $1/f$  noise.

In addition, significant drifts as well as  $1/f$  noise produced by leakage currents of the reference electrode have been found [Jakobson et al. \(2000\)](#). These currents can influence operation due to parasitic paths to the device or the measurement setup. Considering a basic potentiometric setup, properly working reference and sensing electrodes should cause no leakage current. However, if this current is present and it does not flow through the gate electrode, there must be a parasitic current path between the reference and electrical parts of the sensor that are immersed in the solution. The leakage currents might lead to serious experimental artifacts and even electrolysis, depending on the electrolyte composition and potentials applied to the system [Janata \(2012\)](#). Interestingly, a recent study reports a correlation between the leakage current of the reference electrode and the direction of the drift [Sohbati and Toumazou \(2015\)](#). By measuring this leakage, the drift could be at least partially predicted and compensated.

One widely neglected issue in most FET-based sensing applications is the requirement of a stable reference electrode. The reference should provide a constant and stable potential during operation as it is indistinguishable from any change in the detectable chemical potential. To date, reference electrodes are still bulky and often fragile. Nevertheless, a notable performance has been recently achieved with Ag/AgCl elements covered with a mixture of KCl salt and a polymer [Vanamo \(2013\)](#). This reference electrode remains within  $\pm 0.5$  mV in 0.1 M KCl for over two months and has a high stability against changes in electrolyte concentration.

### 3.2. Scaling laws

The scaling laws are an important aspect to consider as they can guide to the proper design of miniaturized sensor structures. In biosensors, the effects of electrode size on the overall response are not well understood. However, miniaturized electrodes are generally considered for better sensitivity in the nanoscale [Zhang et al. \(2016\)](#), whereas the potentiometric devices are considered scaling invariant for typical sizes [Madou and Cubicciotti \(2003\)](#). Many analytes are present in extremely low copy number in a real sample, and measuring a low concentration in low volumes presents a challenge by itself and some of the reported extremely low detection limits has been called into question [Chen \(2013\)](#); [Squires et al. \(2008\)](#). This is caused by the improbability of the charged complex in finding the sensing surface for binding because the theoretically predicted time scales for binding can be on the order of days.

The scaling laws have been analyzed using stochastic differential

methods where the probability distributions are computed as functions of time [Das et al. \(2009\)](#). Contrary to the common belief, the size reduction of the sensing electrode is considered to significantly decrease the achievable SNR and dynamic range, and the overall benefits of excessive size reduction are questioned.

Experimental verification with SiNW sensors has revealed that a small nanowire diameter improves sensitivity, whereas an increase in the number of parallel wires reduces sensitivity [Li et al. \(2011\)](#). However, a CMOS-based modeling study found a clear advantage of increasing the number of pixels per spot [Couniot et al. \(2012\)](#), namely, the detection limit and the resolution are improved without significantly affecting the SNR or sensitivity. The combination of these results seems to indicate that there is a great variety of biosensors and methods to study them, and it is difficult to draw generalized conclusions.

With ISEs, however, theory and models relating size and performance exist [Bobacka et al. \(2008\)](#). In electrochemical sensors, it is important to understand the fundamental property that the measured chemical target is not mostly electrical but, for example, ionic. Moreover, all such ISEs, including the reference electrode, are asymmetric in the sense that the ions do not enter the electronic readout device. Therefore, at some point in the system, transduction should occur from an ionic to an electrical signal via a reversible redox reaction. A common redox reaction occurring in an Ag/AgCl electrode in contact with chloride ions reads [Bobacka et al. \(2008\)](#)



The ion-to-electron transduction is analogous to the above reaction for different materials, such as polyaniline. The electrodes have a finite amount of redox-sensitive material, which leads to finite redox capacitance  $C$  and can be presented as

$$\frac{\Delta V}{\Delta t} = \frac{i}{C}, \quad (3)$$

where  $i$  is a constant current and  $V$  is the electrode potential varying over time  $t$ . Capacitance  $C$  is complemented with a small series resistance  $R$  that shifts the potential by a constant amount:

$$\Delta V = iR. \quad (4)$$

This simple RC model reveals the main principle underlying ion-to-electron transduction. In high-impedance potentiometers, current induced potential differences can be neglected, but currents induced by electrical noise may lead to changes in the measured potential. In addition, when electrodes are miniaturized, resistance  $R$  tends to increase and capacitance  $C$  to decrease, leading to reduced potential stability [Bobacka et al. \(2008\)](#). However, solid-contact microelectrodes have been successfully employed, for example, to measure the Martian soil for various ion concentrations [Kounaves et al. \(2002\)](#) as well as the potassium concentration in a rodent brain [Odijk et al. \(2015\)](#). Miniaturization obviously makes the construction of arrays more sensible and such configurations have shown to overcome some selectivity limits of single sensors [Mourzina et al. \(2001\)](#).

A common practice in biosensing is to replace the bulky reference electrode by inert metals such as Pt or Au. However, the electrode reactions of these materials are not well defined, and therefore using them for gating the device can result in significant potential instabilities [Chen \(2013\)](#). In addition, it is common to use Au as the sensing gate with some functionalization towards biochemical reactions. Nevertheless, such electrodes usually present significant drifts in potentiometric applications [Kamahori et al. \(2008\)](#).

### 3.3. Double-layer screening

A widely debated issue is the label-free detection of biomolecules. Originally, it was believed that the fact of biomolecules carrying intrinsic charge allowed their detection using field-effect devices.

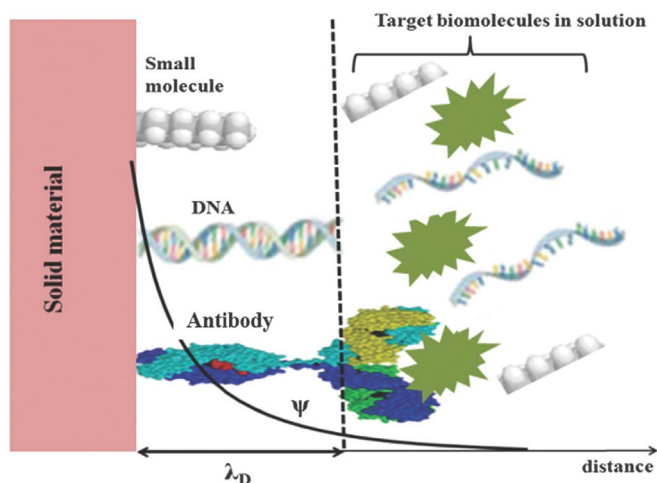


**Fig. 5.** Electrical double-layer length in the presence of different targets (dimensions are not scaled). Reprinted with permission from Huang et al. (2015). Copyright 2015 Royal Society of Chemistry.

Despite significant efforts, the results did not prove satisfactory due to the electrical double layer Schasfoort et al. (1990). For instance, in ionic solutions, the small ions, which carry an opposite charge to that of the detectable large macromolecule, screen the observed net charge by a cloud of opposite charge around the macromolecules. Screening is dependent on the distance between the surface and the point of observation. The amount of observed charge is characterized by the Debye screening length. At a distance of one Debye length, the electrical signal decays to  $1/e$  of its original value Israelachvili (2011). Typical screening lengths are in the order of 1 nm unless very diluted solutions are considered. This is considered to be the main reason limiting the label-free biosensor development Huang et al. (2015). Fig. 5 depicts the electrical double-layer length compared to the size of several biomolecules; the larger the molecule, the stronger the screening effect. Additionally, linking the capture molecule to the surface commonly requires some linker molecules that further increase the distance to the target molecule.

Recently, the origins for improved nanowire biosensors have been investigated using finite-element simulations Shoorideh and Chui (2014). Research concludes that the high surface-to-volume ratio, which is commonly used to explain improved sensitivity, is incorrect. In contrast, the improvement is found to result from the nanoscale surface geometry rather than from a miniature FET itself. More specifically, the counter-ion screening is stronger near convex surfaces than near concave surfaces. Although the nanowire has a convex shape, when it lies on an insulating substrate the corners create a concave surface. It is intuitively explained that the more the electrolyte surrounds the surface, the stronger the screening will be. It is also noteworthy that the sensitivity depends on the wire radius, and it improves when the radius approaches a Debye length. Therefore, the screening caused by the double-layer capacitance varies with the electrode geometry. This offers an explanation for the improved sensitivity of nanowire FETs that contradicts the common belief. Other studies present similar screening simulation results Srensen et al. (2007) and double-layer capacitance values Wang and Pilon (2011); Dickinson and Compton (2009). Furthermore, screening is an interfacial property and indicates that if the FET structure is properly designed it should not critically affect the sensitivity.

A study related to those mentioned above considers the combination of a SiNW and a MOSFET. This hybrid sensor uses a nanowire as the recognition element and a MOSFET as the transducer. The SiNW drain is connected to the MOSFET gate, and a constant current is driven through the SiNW. Then, the conductance variations of the SiNW are seen at the MOSFET gate as potential changes. The study

concludes that a significant amplification in the current response is obtained for both pH and charged-polymer detection compared to using a single SiNW Lee et al. (2015), and indicates the advantage of combining the best characteristics of nanoscale interfaces and existing transistors.

### 3.4. Sensitivity improvement

Several attempts to improve sensitivity include using either different sensor architectures Zhang and Lieber (2016); Maddalena et al. (2008) or electromechanical coupling Jain et al. (2012), and directly engineering the sensing surface Zhang et al. (2015a); Gao et al., (2015, 2016). These studies focus on overcoming the screening effects and include both electric-field-based enhancement as well as direct interfacial modifications.

A straightforward modification was achieved by combining a FET-based sensor with alkaline phosphatase labels that induced Ag precipitation, yielding to a detection free of Debye screening Jang et al. (2015). This adds complexity to the system because it uses labels, but label-based detection is well established and robust. Moreover, the detection limit is claimed to be lower than with conventional ELISA. Another approach for enhanced immunosensing involves the use of a small-receptor antigen-binding fragment as a probe that is significantly smaller than a whole antibody Cheng et al. (2014).

Field-effect sensors can also be driven with an AC excitation signal. When the frequency is high enough, the ions in the solution are unable to form the double layer after the AC perturbations. This allows probing further into the solution, and it also decreases the sensitivity towards small absorbates within the double layer Lemay et al. (2016). This type of electrochemical impedance spectroscopy has been recently used in a CMOS nanocapacitor array to detect living cells Real-time imaging (2015), but the detection principle is general and has been used for different analytes and applications with conventional electrodes Lisdat and Schäfer (2008); Pejic and Marco (2006). The nanocapacitor array is manufactured using CMOS, where two transistors charge and discharge the sensing electrode at a high frequency (see Fig. 6) Real-time imaging (2015); Lemay et al. (2016). This leads to a detectable average current that changes depending on the charge resting on the electrode. A proof-of-concept detection was achieved using 2.5  $\mu\text{m}$  diameter microparticles. The high-frequency method effectively mitigates the electric double-layer screening. This general detection platform has been pursued by NXP Semiconductors.

Other methods based on high frequencies that rely on the electric

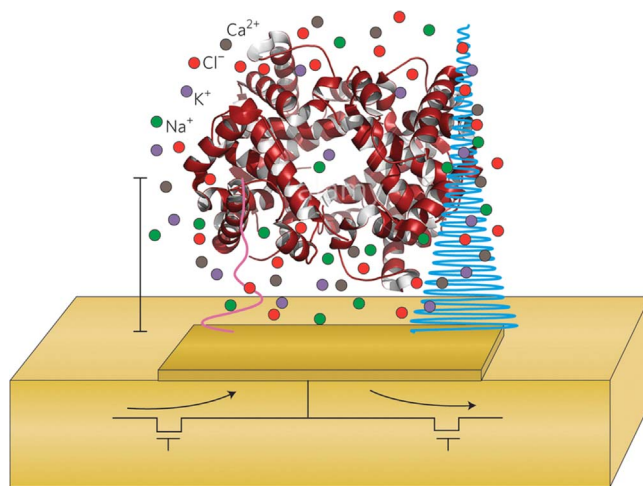


**Fig. 6.** Illustration of a nanocapacitor electrode that is charged and discharged at a high frequency using two metal-oxide-semiconductor transistors, allowing detection beyond the Debye limit. The detectable charge lies on the surface of the nanocapacitor Ingebrandt (2015). Copyright 2015 Nature Publishing Group.

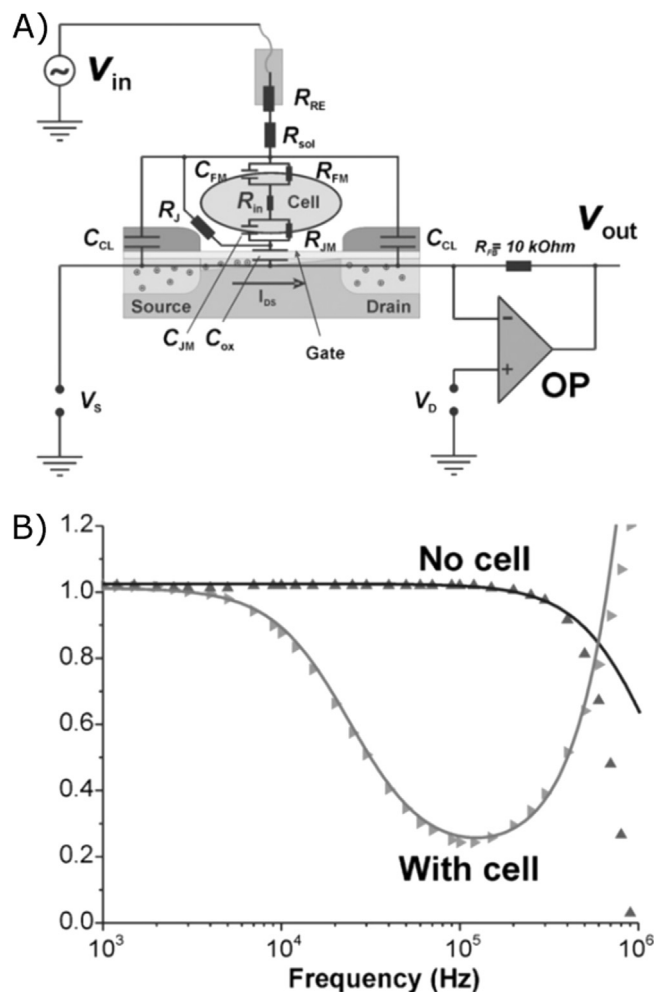


**Fig. 7.** A) Equivalent circuit of a FET-based sensor with AC excitation at the reference electrode. The readout is achieved using phase-selective amplifiers. B) Example of transfer curves obtained for frequencies from 1 kHz to 1 MHz Schäfer et al. (2009). Copyright 2009 Elsevier.

double-layer breakdown have been successfully used for the detection of single-nucleotide polymorphisms and cells without requiring labels Ingebrandt et al. (2007); Schäfer et al. (2009); Susloparova et al. (2015). This type of techniques typically uses a sinusoidal component with an amplitude of 10 mV fed into the reference electrode and swept from 1 kHz to 1 MHz, as illustrated in Fig. 7. The output is read using lock-in amplifiers. The drawback of high-frequency detection is the delicate and complex electronics required to both drive the device and read the sensor output. Still, the superimposed AC excitation signal has shown improvements in DNA sensor stability with gold electrodes. More specifically, the AC signal reduced the time required to stabilize the sensor Kamahori et al. (2008). However, the possible sensitivity improvement was not discussed, and the readout scheme focused on the detection of baseline change rather than on the AC signal, simplifying the detection.

A modification of a nanowire FET-gate interface with a porous and biomolecule-permeable polymer layer was used to increase the effective Debye screening length and thus the sensitivity in label-free detection Gao et al., (2015, 2016). This strategy is general and should be applicable beyond nanowire FETs.

An enhanced response has also been reported by using a hydrophobic passivation layer around the active region compared to the same structure with hydrophilic passivation. This modification is reported to yield a 100× sensitivity improvement Kim et al. (2013). The results indicate that the binding probability is increased when the

fluid is more strictly confined on top of the sensing area.

#### 4. Detection mechanisms using FETs

This section covers the most important detection mechanisms for FET sensors such as pH and ion detection as well as direct and indirect biosensing. Moreover, the recent additions to the theories and state-of-art are reviewed.

##### 4.1. pH sensitivity of oxide interfaces

Oxides are inherently pH-sensitive surfaces and one of the most experimentally studied and modeled surfaces van Hal et al. (1995); Martinoia and Massobrio (2000); Georgiou and Toumazou (2009). The pH response was originally described using the Nernst equation, but experiments commonly exhibit sub-Nernstian slopes. More advanced theories consider a double layer that describes the electrolyte solution as a capacitance, and the surface charge is explained through the site-binding model. It was realized that the simple capacitor equation,  $\Psi_0 = \sigma_0 / C_{DL}$ , yields results close to those experimentally observed van Hal et al., (1995, 1996). Subsequent efforts are usually either modifications or extensions to the well-established theory, summarized as follows Jayant et al. (2013a):

$$\frac{\partial \Psi_0}{\partial p H_B} = -2.3 \frac{kT}{q} \left( \frac{1}{1 + \alpha} \right), \quad (5)$$

$$\alpha = \left( \frac{2.3kT C_{DL}}{q^2 \beta_{int}} \right), \quad (6)$$

$$\beta_{int} = 2.3 H_S^+ N_S \frac{K_B H_S^{+2} + 4K_A K_B H_S^+ + K_A K_B^2}{(K_A K_B + K_B H_S^+ + H_S^+)^2}, \quad (7)$$

$$C_{DL} = \frac{C_{diff} C_{Stem}}{C_{diff} + C_{Stem}}. \quad (8)$$

The sensitivity coefficient,  $\alpha$ , can have values from 0 to 1. From the equations above, we observe that a Nernstian slope requires a high buffering capacity,  $\beta_{int}$ . The buffer capacity is strongly dependent on the density of the ionizable groups,  $N_S$ , and has a key role in determining the slope of the pH response. The high buffer capacity is achieved by either a high ionizable-group density or a small separation between the surface dissociation constants,  $\Delta pK = pK_B - pK_A$ . For pH-sensitive ISFETs, the high buffering capacity also minimizes the effect of the electrolyte ionic strength. Capacitance  $C_{DL}$  also influences the  $pH_B$  sensitivity, but it has only a modest effect with a high buffering capacity. For sub-Nernstian surfaces, the impact can be more significant; however, such surfaces provide the ability for electric-field control over the fluidic part Kaisti et al. (2015a).

A recent addition to this theory considers the finite counter-ion size Kilic et al. (2007) as a parameter affecting the  $pH_B$  sensitivity Parizi et al. (2017). The  $pH_B$  sensitivity equation can be modified as

$$\frac{\partial \Psi_0}{\partial p H_B} = -2.3 \frac{kT}{q} \left( \frac{1}{1 + \alpha - \delta} \right), \quad (9)$$

$$\delta = \frac{2a^3 c_B \sinh\left(\frac{q\Psi_0}{kT}\right)}{1 + 4a^3 c_B \sinh^2\left(\frac{q\Psi_0}{2kT}\right)}, \quad (10)$$

where  $c_B$  is the counter-ion bulk concentration and  $a$  is the ion size. The Nernst limit (i.e., 59 mV/pH<sub>B</sub>) originating from the classic Boltzmann relation is due to the point-charge assumption without considering the physical size. The ions saturate near the surface after a certain potential, and subsequently the counter-ions repel each other creating a wider diffusion layer. This crowding effect results in a higher

hydrogen ion concentration at the surface, explaining the increased  $\text{pH}_b$  sensitivity for large counter-ions (ca. 10 Å). This can be seen from the modified  $\text{pH}_b$  sensitivity equation incorporating size-dependent sensitivity parameter  $\delta$  Parizi et al. (2017).

Measuring pH is a routine practice, important in many chemical processes. A recent work uses it for point-of-care diagnostics Toumazou et al. (2013). The detection scheme employs an on-chip polymerase chain reaction (PCR) and detects the released hydrogen ions when nucleotides are incorporated to the growing DNA strands. The local temporal shift in the  $\text{H}^+$  concentration results in a change in the ISFET surface potential. The use of PCR creates a large number of DNA templates and thus, simultaneous nucleotide incorporations. This subsequently creates a sufficient change on the hydrogen ion concentration for detection. The amplification is highly effective as the amount of DNA strands grows exponentially. The specificity of the system is obtained from a primer that is required to initiate the PCR and can be designed to bind a specific target. This detection scheme using pH as the indicator is also found in the Ion Torrent next generation sequencer Rothberg et al. (2011).

#### 4.2. Ion detection using chemFETs

When ISFETs are modified to be chemically sensitive to ions other than  $\text{H}^+$ , they are called ChemFETs Schoning and Poghossian (2002). The key component that determines the selectivity of the target over other interfering ions is the ISM, which creates a nonpolarized interface with the solution. Ideally, the interface is only permeable to a specific ion, but in practice, interfering ions create an additional charge transfer over the membrane, thus limiting the selectivity and increasing the detection limit. The electrochemical cell potential can be expressed by the Nikolsky-Eisenman equation:

$$V_{\text{cell}} = V_{\text{cell}}^0 + \frac{RT}{z_i F} \ln(a_i + K_{i,j} a_j^{z_i/z_j} + L), \quad (11)$$

where  $a$  is the activity ( $i$  for the primary ion and  $j$  for the interfering ion),  $K_{i,j}$  is the selectivity coefficient,  $L$  represents the detection limit,  $z$  is the valence of a specific ion, and  $R$ ,  $T$ , and  $F$  are the gas constant, the temperature, and the Faraday constant, respectively. This extended version of the Nernst equation allows the estimation of the sensor selectivity and detection limit when parameters  $K_{i,j}$  and  $L$  are obtained experimentally Bobacka et al. (2008). By neglecting both the interfering ions and detection limit, the expression reduces to the Nernst equation. Hence, the resemblance to ISFET formulations is clear as in principle they are the same.

ISEs have been applied in many fields including biomedical and environmental monitoring. In many cases, they provide excellent performance compared to other types of sensors. The measurement of biologically relevant electrolytes in body fluids is still a key development area for ISE research, and billions of measurements are performed globally each year. Additionally, potentiometric sensors measure the ion activity rather than its concentration. This is beneficial for health-related applications in which health disorders are commonly related with this activity Zhang et al. (2008).

Current trends in research aim to develop new ionophores with increased selectivity and lipophilicity by using ISEs in direct contact with blood samples Vanamo (2013); Abramova et al. (2009). In addition, the miniaturization of analyzers and solid-state reference electrodes is required for fully integrated sensor constructions. Moreover, although ChemFETs are a suitable technology for transduction, they are not yet commercially available for clinical chemistry applications. Common challenges include the encapsulation of the FET and insufficient adhesion of polymer membranes to the gate Abramova et al. (2009).

Recent ChemFET-related publications include a miniaturized multi-sensor chip for direct detection of pH, potassium, sodium, and chloride ions in blood serum Abramova et al. (2009). The selectivity

was achieved using ISMs. The same technique was applied to the analysis of natural mineral water and its applicability for sensing in real samples was verified Ipatov et al. (2008). Ion-channel screening of cells with a ChemFET array Walsh et al. (2014) and detection of *E. coli* bacteria via potassium-sensitive FETs on a CMOS chip Nikkhoo et al. (2013) have also been demonstrated.

#### 4.3. Indirect detection of macromolecules

The use of redox-sensitive surfaces and labels is a straightforward approach that substantially reduces the screening associated with methods based on intrinsic charge. Usually, enzyme labels can be used to react with the sensing surface. For example, in DNA detection, ferrocenyl-alkanethiol-modified gold electrodes exhibit a larger dynamic range and significantly improved long-term drift compared to the direct detection mechanism Nakazato (2013). Furthermore, a common practice for antigen detection is to conjugate an enzyme label to a secondary antibody that specifically binds to the detected antigen Zhang et al. (2015b). The label reacts with the surface through electron transfer. However, this practice, beneficial to achieve more robust sensing, generally requires more complicated sample preparations and measurement devices.

Enzymes can also function directly as the recognition layer. Enzyme FETs are usually created by immobilizing an enzyme onto the FET gate. For the immobilization, several techniques are available, such as physical and chemical absorption, entrapment within polymeric matrices, covalent binding, cross-linking, and mixed physicochemical methods Schoning and Poghossian (2002). The first enzyme-based ISFET was created by depositing a membrane on the gate with cross-linked penicillinase. When penicillin is present in the sample, the enzyme catalyzes the hydrolysis of penicillin into penicilloic acid. Next, protons that are released during the reaction change the pH near the gate, and this change can be detected van der Schoot and Bergveld (1987); Dzyadevych et al. (2006).

An alternative for pH-based enzymatic reaction sensing can be achieved with organic polymers that accommodate effective electron-transfer properties, thus allowing the direct detection of enzymatic or redox reactions Purvis et al. (2003). In this type of detection, additional mediators are not required for electron transfer. This can be used for creating simple sensing systems towards standalone devices Dhand (2011).

#### 4.4. Direct detection of macromolecules

##### 4.4.1. Detection of oligonucleotides

An oligonucleotide is a much smaller macromolecule than a protein. Thus, the Debye screening effect does not as strongly affect its detection Fig. 8. This has attracted significant interest in the scientific community given the potential for label-free detection in molecular diagnostics Poghossian and Schöning (2014). A DNA-FET based on an oligonucleotide probe, shown in Fig. 9, can be constructed by immobilizing specific probes on the transistor gate. The complementary target probe hybridizes with high specificity to the probe. Therefore, highly selective sensors can, at least in theory, be constructed. The negatively charged DNA backbone creates a potential shift at the sensing gate upon detection. The length of the DNA bases is about 0.34 nm; consequently, at least a part of the charge from the hybridized DNA complex is seen at the gate surface with practical salt concentrations that allow sufficient hybridization efficiency Shen et al. (2003).

A sample can contain several important targets to be detected. Transistor-based sensors are especially well suited for the multiplexed detection of several targets in a single reaction as the sensing elements can be constructed to have an almost independent operation. This operation is achieved by incorporating several transistors in a single array with different DNA probes. Several studies have demonstrated label-free detection based on hybridization of DNA probes using



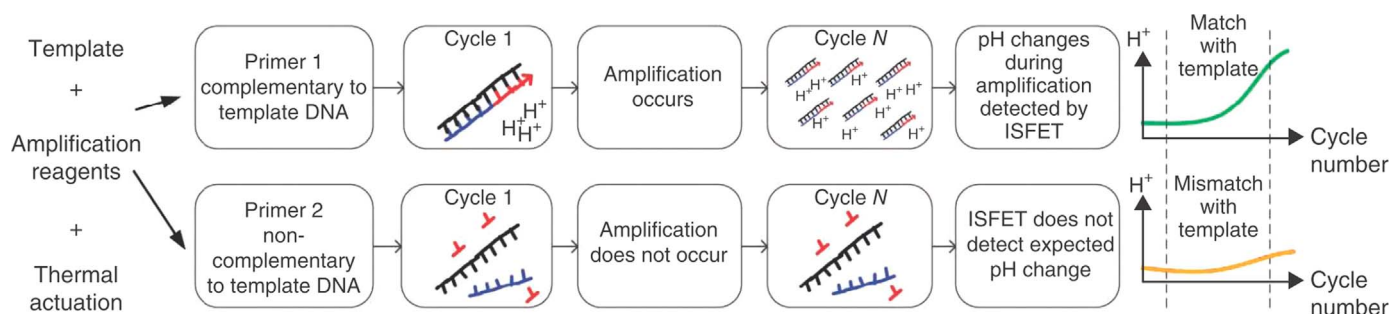


**Fig. 8.** Illustration of a label-free real-time system based on pH detection. The DNA amplification procedure releases hydrogen ions when nucleotides are incorporated to the growing double strand. This chemical reaction is detected using ISFETs [Toumazou et al. \(2013\)](#). Copyright 2013 Nature Publishing Group.

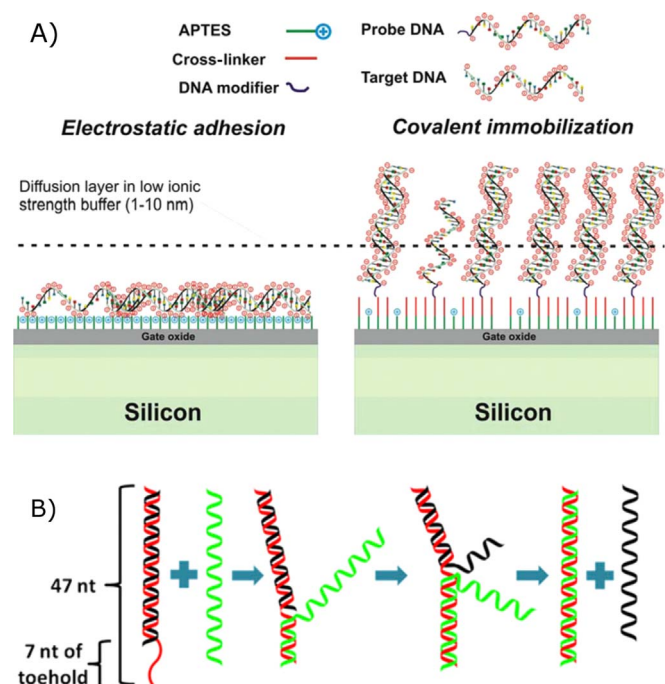


**Fig. 9.** The basic approaches for DNA immobilizations include: A) electrostatic immobilization where the probe lies flat on the surface (left), and covalent attachment at one end of the probe (right) [Pachauri and Ingebrandt \(2016\)](#). B) Approach for enhanced specificity. The double-stranded probe contains one probe attached to surface and a weakly bounded complementary strand. The weak strand is replaced when a perfect-match target is present in the sample solution [Hwang et al. \(2016\)](#).

miniaturized transistor systems [Uslu et al. \(2004\)](#); [Ishige et al. \(2006\)](#); [Song et al. \(2006\)](#); [Kamahori et al. \(2008\)](#); [Hwang et al. \(2016\)](#); [Xu et al., \(2014, 2015\)](#); [White et al. \(2015\)](#) as well as detection based on direct hybridization using DNA arrays [Nakazato \(2009\)](#); [Barbaro et al. \(2012\)](#); [Blin et al. \(2014\)](#).

[Fig. 9-A](#) illustrates two direct hybridization methods. The method shown on the left of the figure is based on electrostatic adhesion [Pachauri and Ingebrandt \(2016\)](#). In this method, the target lies mostly within the electric double layer, and a clear potential shift on the immobilization is usually observed. However, the hybridization is usually considered as suboptimal because the target needs to wound around the probe. However, the method shown on the right of [Fig. 9-A](#) is based on a probe with one end covalently attached to the surface. In this method, a smaller portion of the target is within the electric double layer, but the hybridization is not severely hindered as in the case of the previous method. Nevertheless, one study found sufficient hybridization affinities for biosensing in both methods [De et al. \(2013\)](#).

An interesting approach for improved signal quality lies in the use of a peptide nucleic acid (PNA) probe. Given the neutral-charge backbone of the PNA, it is expected to yield enhanced detection as

the electrostatic repulsion between the probe and target is eliminated, and hybridization can be achieved in lower salt concentrations [Goda et al. \(2013\)](#). The use of these probes have also been theoretically found to have a clear benefit for transduction of the hybridization signal [Liu and Dutton \(2009\)](#).

Recently, a method for improved specificity has been considered [Hwang et al. \(2016\)](#). A detection scheme for single-nucleotide polymorphisms was demonstrated, where a double-stranded probe is utilized as shown in [Fig. 9-B](#). One strand is attached to the surface and has a weakly binding complementary strand attached to it. A specific toehold region of 7 base pairs, starting from the surface end, is left as a single strand. The weak strand is replaced when a perfect-match strand is present in the sample. In case of a nonperfect match, such as a strand with a single-nucleotide polymorphism, the replacement either does not take place or is hindered due to the weak strand already in place.

Although label-free detection has been reported on numerous occasions, a critical review concluded that there is a wide variability of empirical results about the changes in the gate potential resulting from the DNA hybridization [Poghossian et al. \(2005\)](#). Moreover, the theoretical understanding was considered to be inadequate to explain the results. This report was presented more than a decade ago, but the fundamental understanding behind the observed measurement results still remain unclear [Poghossian and Schöning \(2014\)](#).

#### 4.4.2. Detection of proteins

Similar to the detection of nucleotides, the direct label-free detection of antibody–antigen interactions has also attracted significant interest. Proteins are usually charged molecules with the exception of certain characteristic pH levels where they carry zero net charge. Given its intrinsic charge, it was originally thought that these molecules could be detected via surface-charge sensing devices. Whether this is possible has been debated. The reason for unsuccessful detection has been considered to be the double-layer screening [Chen \(2013\)](#); [Schasfoort et al. \(1990\)](#). However, several reports claim successful label-free detection even in cases where the size of the complex, such as an antibody–antigen complex, is at vastly longer distances than the electric double layer [Poghossian and Schöning \(2014\)](#).

A common explanation for these observed results is the Donnan effect [Chen \(2013\)](#). According to this theory, proteins are considered as a membrane on the electrode surface. In addition, small ions can shuffle between the solution and this protein membrane. Then, when a fixed charge is present due to the target, a difference of ion concentration appears on the interface between the membrane and the solution. This redistribution of ions creates a detectable change in the interfacial potential. Moreover, the change in this Donnan potential also causes a shift in pH. Thus, the total response is the combination of the surface pH response and the Donnan potential. This theory also states that a Nernstian surface fully compensates the changes induced by the protein binding, and a non-Nernstian surface is required for successful detection [Schasfoort et al. \(1990\)](#); [Chen \(2013\)](#).

## 5. Discussion and conclusion

ISFETs were introduced in the 1970s by Bergveld (1970) and have since received significant attention. The first commercial application was a pH ISFET sensor Bergveld (2003) that are sold commercially by several companies (e.g., Thermo Fisher Scientific–USA, Sentron–Netherlands, Microsens–Switzerland, Honeywell–USA, D+T Microelectronica–Spain). More recently, the Ion Torrent technology that utilizes massively parallel CMOS arrays with pH-sensitive ISFETs has entered the next generation sequencing market and competes with the more established optical systems Rothberg et al. (2011).

Despite significant efforts, the overall progress towards commercial miniaturized and multiplexed devices has been modest. Encapsulation of electronics for wet environments has created a significant difficulty for mass-producible sensors. In laboratory settings, such encapsulations have been demonstrated successfully on numerous occasions, but their applicability for mass production, especially if an aqueous storage medium is required, remains unclear Huang et al. (2015). Additionally, although these sensors provide the promise of being low-cost and simple sensors, every application requires more than a sensor to reach the end device. For example, real samples of complex mixtures containing various biological species present great challenges for a specific detection Wei et al. (2010). Moreover, several pretreatment processes might be required before performing the actual detection. Only a very limited number of analytes can be measured directly from the sample such as the case of blood glucose, which has resulted in the most successful electrical biosensor (i.e., amperometric) so far. Furthermore, several factors such as ionic strength, pH level, temperature, or even lightning could create variability in the detection.

Regardless of the challenges, several companies are aiming to release point-of-care tests in the near future. For instance, DNAe is currently developing a sepsis test based on ISFET manufactured using unmodified CMOS processes.<sup>1</sup> The detection is based on detecting the hydrogen ions that are released during DNA amplification, as described in Section 4.1. The detection principle is general and other tests can be created when accompanied with a suitable sample preparation. In addition, Quantum MDx is anticipating to launch its handheld molecular diagnostics Q-POC device in 2018.<sup>2</sup> This device originally intended to use licensed SiNW sensor technology as the transducer Cui and Lieber (2001). Currently, the company informs that the target DNA hybridization is detected via fluorescence methods. InSilixa is developing a general platform for molecular diagnostic tests using a CMOS biochip.<sup>3</sup> The current detection modalities are based on fluorescence, bioluminescence, voltammetry, and impedance measurements that can be used to diagnose a broad range of diseases.

Although the commercial success has been somewhat modest, there are currently several promising attempts for successful tests. Since the invention of ISFET in the 1970s, the research has been concentrated for a long time on pH detection, and the most successful solutions are currently based on it. In the near future, perhaps other sensing modalities will become mature towards scientific and commercial success.

## Acknowledgements

This work was supported by the Jenny and Antti Wihuri Foundation, Tekniikan edistämissäätiö, and Finnish Funding Agency for Innovation (Tekes) under grant 1563/31/2016.

## References

- L.C., P.F., V.A., L.S.G., S.L., J.M.A., W.F.P., 2015. Real-time imaging of microparticles and living cells with cmos nanocapacitor arrays, *Nat Nano*.
- Abramova, N., Ipatov, A., Levichev, S., Bratov, A., 2009. Integrated multi-sensor chip with photocured polymer membranes containing copolymerised plasticizer for direct ph, potassium, sodium and chloride ions determination in blood serum, *Talanta*. In: *Proceedings of the 15th International Conference on Flow Injection Analysis*, Nagoya, Japan, 28 September - 3 October 2008, 79, pp. 984–989.
- Ahmad, F., Hashsham, S.A., 2012. Miniaturized nucleic acid amplification systems for rapid and point-of-care diagnostics: a review. *Anal. Chim. Acta* 733, 1–15.
- Aliakbarinodhi, N., Jolly, P., Bhalla, N., Miodek, A., De Micheli, G., Estrela, P., Carrara, S., 2017. Aptamer-based field-effect biosensor for tenofovir detection. *Sci. Rep.* 7.
- Arya, S.K., Wong, C.C., Jeon, Y.J., Bansal, T., Park, M.K., 2015. Advances in complementary metal oxide semiconductor based integrated biosensor arrays. *Chem. Rev.* 115, 5116–5158.
- Bandodkar, A.J., Jeerapan, I., Wang, J., 2016. Wearable chemical sensors: present challenges and future prospects. *ACS Sens.* 1, 464–482.
- Barbaro, M., Bonfiglio, A., Raffo, L., 2006a. A charge-modulated fet for detection of biomolecular processes: conception, modeling, and simulation. *IEEE Trans. Electron Devices* 53, 158–166.
- Barbaro, M., Bonfiglio, A., Raffo, L., Alessandrini, A., Facci, P., Barak, I., 2006b. Fully electronic dna hybridization detection by a standard cmos biochip. *Sens. Actuators B: Chem.* 118, 41–46.
- Barbaro, M., Caboni, A., Loi, D., Lai, S., Homsy, A., van der Wal, P., de Rooij, N., 2012. Label-free, direct dna detection by means of a standard cmos electronic chip. *Sens. Actuators B: Chem.* 171 (172), 148–154.
- Bausells, J., Carrabina, J., Errachid, A., Merlos, A., 1999. Ion-sensitive field-effect transistors fabricated in a commercial cmos technology. *Sens. Actuators B: Chem.* 57, 56–62.
- Bergveld, P., 1970. Development of an ion-sensitive solid-state device for neurophysiological measurements. *IEEE Trans. Biomed. Eng.* BME-17, 70–71.
- Bergveld, P., 2003. Thirty years of ISFETOLOGY: what happened in the past 30 years and what may happen in the next 30 years. *Sens. Actuators B: Chem.* 88, 1–20.
- Blin, A., Cisse, I., Bockelmann, U., 2014. Electronic hybridization detection in microarray format and dna genotyping. *Scientific Reports*.
- Bobacka, J., Ivaska, A., Lewenstam, A., 2008. Potentiometric ion sensors. *Chem. Rev.* 108, 329–351.
- Cattrall, R.W., Freiser, H., 1971. Coated wire ion-selective electrodes. *Anal. Chem.* 43, 1905–1906.
- Chen, S., 2013. *Electronic Sensors Based on Nanostructured Field-Effect Devices*, Ph.D. thesis, Uppsala Universitet.
- Cheng, S., Hotani, K., Hideshima, S., Kuroiwa, S., Nakanishi, T., Hashimoto, M., Mori, Y., Osaka, T., 2014. Field effect transistor biosensor using antigen binding fragment for detecting tumor marker in human serum. *Materials* 7, 2490–2500.
- Couniot, N., Afzaljan, A., Flandre, D., 2012. Scaling laws and performance improvements of integrated biosensor microarrays with multi-pixel per spot. *Sens. Actuators B: Chem.* 166167, 184–192.
- Cui, Y., Lieber, C.M., 2001. Functional nanoscale electronic devices assembled using silicon nanowire building blocks. *Science* 291, 851–853.
- Das, S., Vikalo, H., Hassibi, A., 2009. On scaling laws of biosensors: a stochastic approach. *J. Appl. Phys.* 105, 102021.
- De, A., Souchelnyskiy, S., van den Berg, A., Carlen, E.T., 2013. Peptide nucleic acid (pna)-dna duplexes: comparison of hybridization affinity between vertically and horizontally tethered pna probes. *ACS Appl. Mater. Interfaces* 5, 4607–4612.
- Dhand, C., Das, M., Datta, M., Malhotra, B., 2011. Recent advances in polyaniline based biosensors. *Biosens. Bioelectron.* 26, 2811–2821.
- Dickinson, E.J.F., Compton, R.G., 2009. Diffuse double layer at nanoelectrodes. *J. Phys. Chem. C* 113, 17585–17589.
- Duarte-Guevara, C., Lai, F.-L., Cheng, C.-W., Reddy, B., Salm, E., Swaminathan, V., Tsui, Y.-K., Tuan, H.C., Kalnitsky, A., Liu, Y.-S., Bashir, R., 2014. Enhanced biosensing resolution with foundry fabricated individually addressable dual-gated isfets. *Anal. Chem.* 86, 8359–8367.
- Dzyadevych, S.V., Soldatkin, A.P., El'skaya, A.V., Martelet, C., Jaffrezic-Renault, N., 2006. Enzyme biosensors based on ion-selective field-effect transistors. *Anal. Chim. Acta* 568, 248–258.
- Gao, N., Zhou, W., Jiang, X., Hong, G., Fu, T.-M., Lieber, C.M., 2015. General strategy for biodetection in high ionic strength solutions using transistor-based nanoelectronic sensors. *Nano Lett.* 15, 2143–2148.
- Gao, N., Gao, T., Yang, X., Dai, X., Zhou, W., Zhang, A., Lieber, C.M., 2016. Specific detection of biomolecules in physiological solutions using graphene transistor biosensors. In: *Proceedings of the National Academy of Sciences*, 113, pp. 14633–14638.
- Georgiou, P., Toumazou, C., 2009. ISFET characteristics in cmos and their application to weak inversion operation. *Sens. Actuators B: Chem.* 143, 211–217.
- Goda, T., Singi, A.B., Maeda, Y., Matsumoto, A., Torimura, M., Aoki, H., Miyahara, Y., 2013. Label-free potentiometry for detecting dna hybridization using peptide nucleic acid and dna probes. *Sensors* 13, 2267.
- Guan, W., Rajan, N.K., Duan, X., Reed, M.A., 2013. Quantitative probing of surface charges at dielectric-electrolyte interfaces. *Lab Chip* 13, 1431–1436.
- Hammond, P.A., Ali, D., Cumming, D.R.S., 2005. A system-on-chip digital ph meter for use in a wireless diagnostic capsule. *IEEE Trans. Biomed. Eng.* 52, 687–694.
- Hu, Y., Georgiou, P., 2014. A robust isfet ph-measuring front-end for chemical reaction monitoring. *IEEE Trans. Biomed. Circuits Syst.* 8, 177–185.
- Hu, J., Stein, A., Buhlmann, P., 2016. Rational design of all-solid-state ion-selective

<sup>1</sup> <http://www.dnae.com/> 5.4.2017.

<sup>2</sup> <http://www.quantumdx.com/> 5.4.2017.

<sup>3</sup> <http://www.insilixa.com/> 5.4.2017.

- electrodes and reference electrodes. *TrAC Trends Anal. Chem.* 76, 102–114.
- Huang, W., Diallo, A.K., Dailey, J.L., Besar, K., Katz, H.E., 2015. Electrochemical processes and mechanistic aspects of field-effect sensors for biomolecules. *J. Mater. Chem. C* 3, 6445–6470.
- Huang, Y.J., Lin, C.C., Huang, J.C., Hsieh, C.H., Wen, C.H., Chen, T.T., Jeng, L.S., Yang, C.K., Yang, J.H., Tsui, F., Liu, Y.S., Liu, S., Chen, M., 2015. High performance dual-gate isfet with non-ideal effect reduction schemes in a soi-cmos bioelectrical soc. In: 2015 IEEE International Electron Devices Meeting (IEDM), pp. 29.2.1–29.2.4. <http://dx.doi.org/10.1109/IEDM.2015.7409792>.
- Hwang, M.T., Landon, P.B., Lee, J., Choi, D., Mo, A.H., Glinsky, G., Lal, R., 2016. Highly specific snp detection using 2d graphene electronics and dna strand displacement. *Proc. Natl. Acad. Sci.* 113, 7088–7093.
- Ingebrandt, S., Han, Y., Nakamura, F., Poghossian, A., Schöning, M., Offenhäuser, A., 2007. Label-free detection of single nucleotide polymorphisms utilizing the differential transfer function of field-effect transistors. *Biosens. Bioelectron.* 22, 2834–2840.
- Ingebrandt, S., 2015. Bioelectronics: sensing beyond the limit. *Nat. Nano.*
- Ipatov, A., Abramova, N., Bratov, A., Dominguez, C., 2008. Integrated multisensor chip with sequential injection technique as a base for electronic tongue devices, *Sensors and Actuators B: Chemical* 131, 48–52. Special Issue: Selected Papers from Proceedings of the 12th International Symposium on Olfaction and Electronic Noses/ISOEN 2007 International Symposium on Olfaction and Electronic Noses.
- Ishige, Y., Shimoda, M., Kamahori, M., 2006. Immobilization of dna probes onto gold surface and its application to fully electric detection of dna hybridization using field-effect transistor sensor. *Jpn. J. Appl. Phys.* 45, 3776.
- Ishige, Y., Shimoda, M., Kamahori, M., 2009. Extended-gate fet-based enzyme sensor with ferrocenyl-alkanethiol modified gold sensing electrode, *Biosensors and Bioelectronics*, 24, 1096–1102. Selected Papers from the Tenth World Congress on Biosensors Shanghai, China, May 14–16, 2008.
- Israelachvili, J.N., 2011. *Intermolecular and Surface Forces*. Academic Press, Waltham, Massachusetts, USA.
- Jain, A., Nair, P.R., Alam, M.A., 2012. Flexure-fet biosensor to break the fundamental sensitivity limits of nanobiosensors using nonlinear electromechanical coupling. *Proc. Natl. Acad. Sci.* 109, 9304–9308.
- Jakobson, C.G., Nemirovsky, Y., 1999. 1/f noise in ion sensitive field effect transistors from subthreshold to saturation. *IEEE Trans. Electron Devices* 46, 259–261.
- Jakobson, C., Feinsod, M., Nemirovsky, Y., 2000. Low frequency noise and drift in ion sensitive field effect transistors. *Sens. Actuators B: Chem.* 68, 134–139.
- Jamasb, S., Collins, S., Smith, R.L., 1998. A physical model for drift in ph ISFETs. *Sens. Actuators B: Chem.* 49, 146–155.
- Janata, J., 2012. Graphene bio-field-effect transistor myth. *ECS Solid State Lett.* 1, M29–M31.
- Jang, H.-J., Cho, W.-J., 2014. Performance enhancement of capacitive-coupling dual-gate ion-sensitive field-effect transistor in ultra-thin-body, *Scientific Reports*.
- Jang, H.-J., Ahn, J., Kim, M.-G., Shin, Y.-B., Jeun, M., Cho, W.-J., Lee, K.H., 2015. Electrical signaling of enzyme-linked immunosorbent assays with an ion-sensitive field-effect transistor. *Biosens. Bioelectron.* 64, 318–323.
- Jayant, K., Auluck, K., Funke, M., Anwar, S., Phelps, J.B., Gordon, P.H., Rajwade, S.R., Kan, E.C., 2013a. Programmable ion-sensitive transistor interfaces. I. electrochemical gating. *Phys. Rev. E* 88, 012801.
- Jayant, K., Auluck, K., Funke, M., Anwar, S., Phelps, J.B., Gordon, P.H., Rajwade, S.R., Kan, E.C., 2013b. Programmable ion-sensitive transistor interfaces. II. biomolecular sensing and manipulation. *Phys. Rev. E* 88, 012802.
- Jayant, K., Singhal, A., Cao, Y., Phelps, J.B., Lindau, M., Holowka, D.A., Baird, B.A., Kan, E.C., 2015. Non-faradaic electrochemical detection of exocytosis from mast and chromaffin cells using floating-gate mos transistors. *Sci. Rep.* 5.
- Jiang, Z., Stein, D., 2010. Electrofluidic gating of a chemically reactive surface. *Langmuir* 26, 8161–8173.
- Kaisti, M., Zhang, Q., Prabhu, A., Lehmusvuori, A., Rahman, A., Levon, K., 2015a. An ion-sensitive floating gate fet model: operating principles and electrofluidic gating. *IEEE Trans. Electron Devices* 62, 2628–2635.
- Kaisti, M., Knuutila, A., Boeva, Z., Kvarnström, C., Levon, K., 2015b. Low-cost chemical sensing platform with organic polymer functionalization. *IEEE Electron Device Lett.* 36, 844–846.
- Kaisti, M., Boeva, Z., Koskinen, J., Nieminen, S., Bobacka, J., Levon, K., 2016. Hand-held transistor based electrical and multiplexed chemical sensing system, *ACS Sensors*.
- Kaisti, M., 2017. Field-effect based chemical and biological sensing: theory and implementation, Ph.D. thesis, University of Turku.
- Kalofonou, M., Toumazou, C., 2014. A low power sub uw chemical gilbert cell for isfet differential reaction monitoring. *IEEE Trans. Biomed. Circuits Syst.* 8, 565–574.
- Kamahori, M., Ishige, Y., Shimoda, M., 2008. Detection of dna hybridization and extension reactions by an extended-gate field-effect transistor: characterizations of immobilized dna probes and role of applying a superimposed high-frequency voltage onto a reference electrode. *Biosens. Bioelectron.* 23, 1046–1054.
- Kilic, M.S., Bazant, M.Z., Ajdari, A., 2007. Steric effects in the dynamics of electrolytes at large applied voltages. I. double-layer charging. *Phys. Rev. E* 75, 021502.
- Kim, J.-Y., Choi, K., Moon, D.-I., Ahn, J.-H., Park, T.J., Lee, S.Y., Choi, Y.-K., 2013. Surface engineering for enhancement of sensitivity in an underlap-fet biosensor by control of wettability. *Biosens. Bioelectron.* 41, 867–870.
- Knopfmacher, O., Tarasov, A., Fu, W., Wipf, M., Niesen, B., Calame, M., Schenberger, C., 2010. Nernst limit in dual-gated si-nanowire fet sensors. *Nano Lett.* 10, 2268–2274.
- Kounaves, S.P., Buehler, M.G., Hecht, M.H., West, S., 2002. Determination of Geochemistry on Mars Using an Array of Electrochemical Sensors, pp. 306–319. URL: <http://pubs.acs.org/doi/abs/10.1021/bk-2002-0811.ch016>. doi:10.1021/bk-2002-0811.ch016.
- Lafleur, J.P., Jnsson, A., Senkbeil, S., Kutter, J.P., 2015. Recent advances in lab-on-a-chip for biosensing applications. *Biosens. Bioelectron.*
- Lee, J., Jang, J., Choi, B., Yoon, J., Kim, J.-Y., Choi, Y.-K., Myong Kim, D., Hwan Kim, D., Choi, S.-J., 2015. A highly responsive silicon nanowire/amplifier mosfet hybrid biosensor, *Scientific Reports*.
- Lei, K.-M., Mak, P.-I., Law, M.-K., Martins, R.P., 2016. Cmos biosensors for in vitro diagnosis - transducing mechanisms and applications. *Lab Chip* 16, 3664–3681.
- Lemay, S.G., Laborde, C., Renault, C., Cossetini, A., Selmi, L., Widdershoven, F.P., 2016. High-frequency nanocapacitor arrays: concept, recent developments, and outlook. *Acc. Chem. Res.* 49, 2355–2362.
- Li, L., Liu, X., Qureshi, W., Mason, A., 2011. Cmos amperometric instrumentation and packaging for biosensor array applications. *IEEE Trans. Biomed. Circuits Syst.* 5, 439–448.
- Lisdat, F., Schäfer, D., 2008. The use of electrochemical impedance spectroscopy for biosensing. *Anal. Bioanal. Chem.* 391, 1555.
- Liu, Y., Dutton, R.W., 2009. Effects of charge screening and surface properties on signal transduction in field effect nanowire biosensors. *J. Appl. Phys.* 106, 014701.
- Liu, Y., Georgiou, P., Prodromakis, T., Constandinou, T.G., Toumazou, C., 2011. An extended CMOSISFET model incorporating the physical design geometry and the effects on performance and offset variation. *IEEE Trans. Electron Devices* 58, 4414–4422.
- Maddalena, F., Spijkman, M., Brondijk, J., Fonteijn, P., Brouwer, F., Hummelen, J., de Leeuw, D., Blom, P., de Boer, B., 2008. Device characteristics of polymer dual-gate field-effect transistors. *Org. Electron.* 9, 839–846.
- Madou, M.J., Cubicciotti, R., 2003. Scaling issues in chemical and biological sensors, *Proceedings of the IEEE*, 91, pp. 830–838.
- Martinoia, S., Massobrio, G., 2000. A behavioral macromodel of the ISFET in SPICE. *Sens. Actuators B: Chem.* 62, 182–189.
- Matzue, G., Florea, L., Diamond, D., 2015. Advances in wearable chemical sensor design for monitoring biological fluids. *Sens. Actuators B: Chem.* 211, 403–418.
- Mehrabani, S., Maker, A.J., Armani, A.M., 2014. Hybrid integrated label-free chemical and biological sensors. *Sensors* 14, 5890.
- Milgrew, M., Riehle, M., Cumming, D.S., 2005. A large transistor-based sensor array chip for direct extracellular imaging, *Sensors and Actuators B: Chemical*, 111, 347–353. *EuroSensors XVIII 2004 Proceedings of the 18th European Conference on Solid-State Transducers*.
- Miscourides, N., Georgiou, P., 2015. Impact of technology scaling on isfet performance for genetic sequencing. *IEEE Sens. J.* 15, 2219–2226.
- Mourzina, Y., Schubert, J., Zander, W., Legin, A., Vlasov, Y., Luth, H., Schoning, M., 2001. Development of multisensor systems based on chalcogenide thin film chemical sensors for the simultaneous multicomponent analysis of metal ions in complex solutions. *Electrochim. Acta* 47, 251–258.
- Nakazato, K., 2009. An integrated ISFET sensor array. *Sensors* 9, 8831–8851.
- Nakazato, K., 2013. Potentiometric, Amperometric, and Impedimetric CMOS Biosensor Array, *State of the Art in Biosensors - General Aspects*, Dr. Toonika Rinken (Ed.), InTech. <http://dx.doi.org/10.5772/53319>.
- Nemiroski, A., Christodouleas, D.C., Hennek, J.W., Kumar, A.A., Maxwell, E.J., Fernandez-Abedul, M.T., Whitesides, G.M., 2014. Universal mobile electrochemical detector designed for use in resource-limited applications. *Proc. Natl. Acad. Sci.* 111, 11984–11989.
- Nikkhoo, N., Gulak, P.G., Maxwell, K., 2013. Rapid detection of e. coli bacteria using potassium-sensitive fets in cmos. *IEEE Trans. Biomed. Circuits Syst.* 7, 621–630.
- Odiq, M., van der Wouden, E., Olthuis, W., Ferrari, M., Tolner, E., van den Maagdenberg, A., van den Berg, A., 2015. Microfabricated solid-state ion-selective electrode probe for measuring potassium in the living rodent brain: compatibility with dc-ecg recordings to study spreading depression. *Sens. Actuators B: Chem.* B 207, 945–953.
- Pachauri, V., Ingebrandt, S., 2016. Biologically sensitive field-effect transistors: from isfets to nanofets. *Essays Biochem.* 60, 81–90.
- Parizi, K.B., Xu, X., Pal, A., Hu, X., Wong, H.S.P., 2017. Isfet ph sensitivity: counter-ions play a key role. *Sci. Rep.* 7.
- Pejic, B., Marco, R.D., 2006. Impedance spectroscopy: over 35 years of electrochemical sensor optimization. *Electrochim. Acta* 51, 6217–6229.
- Perumal, V., Hashim, U., 2014. Advances in biosensors: principle, architecture and applications. *J. Appl. Biomed.* 12, 1–15.
- Poghossian, A., Schöning, M.J., 2014. Label-free sensing of biomolecules with field-effect devices for clinical applications. *Electroanalysis* 26, 1197–1213.
- Poghossian, A., Chertvty, A., Ingebrandt, S., Offenhäuser, A., Schoning, M., 2005. Possibilities and limitations of label-free detection of dna hybridization with field-effect-based devices, *Sensors and Actuators B: Chemical*, 111, 470–480. *EuroSensors XVIII 2004 Proceedings of the 18th European Conference on Solid-State Transducers*.
- Privett, B.J., Shin, J.H., Schoenfish, M.H., 2010. Electrochemical sensors. *Anal. Chem.* 82, 4723–4741.
- Prodromakis, T., Liu, Y., Toumazou, C., 2011a. A low-cost disposable chemical sensing platform based on discrete components. *IEEE Electron Device Lett.* 32, 417–419.
- Prodromakis, T., Liu, Y., Yang, J., Hollinghurst, D., Toumazou, C., 2011b. A novel design approach for developing chemical sensing platforms using inexpensive technologies. In: *Biomedical Circuits and Systems Conference (BioCAS)*, 2011, IEEE, pp. 369–372.
- Purvis, D., Leonardova, O., Farmakovskiy, D., Cherkasov, V., 2003. An ultrasensitive and stable potentiometric immunosensor. *Biosens. Bioelectron.* 18, 1385–1390.
- Ronkainen, N.J., Halsall, H.B., Heineman, W.R., 2010. Electrochemical biosensors. *Chem. Soc. Rev.* 39, 1747–1763.
- Rothberg, J.M., et al., 2011. An integrated semiconductor device enabling non-optical genome sequencing. *Nature* 475, 348–352.

- Schäfer, S., Eick, S., Hofmann, B., Dufaux, T., Stockmann, R., Wrobel, G., Offenhäuser, A., Ingebrandt, S., 2009. Time-dependent observation of individual cellular binding events to field-effect transistors, *Biosensors and Bioelectronics*, 24, 1201–1208. Selected Papers from the Tenth World Congress on Biosensors Shanghai, China, May 14–16, 2008.
- Schasfoort, R., Bergveld, P., Kooyman, R., Greve, J., 1990. Possibilities and limitations of direct detection of protein charges by means of an immunological field-effect transistor. *Anal. Chim. Acta* 238, 323–329.
- Schoning, M.J., Poghosian, A., 2002. Recent advances in biologically sensitive field-effect transistors (biofets). *Analyst* 127, 1137–1151.
- Shen, N.Y.-M., Liu, Z., Lee, C., Minch, B.A., Kan, E.C.-C., 2003. Charge-based chemical sensors: a neuromorphic approach with chemoreceptive neuron mos (CvMOS) transistors. *IEEE Trans. Electron Devices* 50, 2171–2178.
- Shoorideh, K., Chui, C.O., 2012. Optimization of the sensitivity of fet-based biosensors via biasing and surface charge engineering. *IEEE Trans. Electron Devices* 59, 3104–3110.
- Shoorideh, K., Chui, C.O., 2014. On the origin of enhanced sensitivity in nanoscale fet-based biosensors. *Proc. Natl. Acad. Sci.* 111, 5111–5116.
- Sohbati, M., Toumazou, C., 2015. Dimension and shape effects on the isfet performance. *IEEE Sens. J.* 15, 1670–1679.
- Song, K.-S., Zhang, G.-J., Nakamura, Y., Furukawa, K., Hiraki, T., Yang, J.-H., Funatsu, T., Ohdomari, I., Kawarada, H., 2006. Label-free dna sensors using ultrasensitive diamond field-effect transistors in solution. *Phys. Rev. E* 74, 041919.
- Spijkman, M., Smits, E.C.P., Cillessen, J.F.M., Biscarini, F., Blom, P.W.M., de Leeuw, D.M., 2011a. Beyond the nerst-limit with dual-gate zno ion-sensitive field-effect transistors. *Appl. Phys. Lett.* 98, 043502.
- Spijkman, M.-J., Myny, K., Smits, E.C.P., Heremans, P., Blom, P.W.M., de Leeuw, D.M., 2011b. Dual-gate thin-film transistors, integrated circuits and sensors. *Adv. Mater.* 23, 3231–3242.
- Squires, M., Messinger, R.J., Manalis, S.R., 2008. Making it stick: convection, reaction and diffusion in surface-based biosensors. *Nat. Biotech.* 26, 417–426.
- Srensen, M.H., Mortensen, N.A., Brandbyge, M., 2007. Screening model for nanowire surface-charge sensors in liquid. *Appl. Phys. Lett.* 91, 102105.
- Streetman, B.G., Banerjee, S.K., 2006. *Solid State Electronic Devices*. Pearson Prentice Hall, New Jersey, USA.
- Susloparova, A., Koppenhofer, D., Law, J.K.Y., Vu, X.T., Ingebrandt, S., 2015. Electrical cell-substrate impedance sensing with field-effect transistors is able to unravel cellular adhesion and detachment processes on a single cell level. *Lab Chip* 15, 668–679.
- Tarasov, A., Gray, D.W., Tsai, M.-Y., Shields, N., Montrose, A., Creedon, N., Lovera, P., O'Riordan, A., Mooney, M.H., Vogel, E.M., 2016. A potentiometric biosensor for rapid on-site disease diagnostics. *Biosens. Bioelectron.* 79, 669–678.
- Toumazou, C., et al., 2013. Simultaneous DNA amplification and detection using a pH-sensing semiconductor system. *Nat. Methods* 10, 641–646.
- Uslu, F., Ingebrandt, S., Mayer, D., Bocker-Meffert, S., Odenthal, M., Offenhäuser, A., 2004. Label-free fully electronic nucleic acid detection system based on a field-effect transistor device. *Biosens. Bioelectron.* 19, 1723–1731.
- Vaknin, O., Khamaisi, B., Mizrahi, M., Ashkenasy, N., 2011. Controlling field-effect transistor biosensor electrical characteristics using immunosorbent assay. *Electroanalysis* 23, 2327–2334.
- van der Schoot, B.H., Bergveld, P., 1987. Isfet based enzyme sensors. *Biosensors* 3, 161–186.
- van der Spiegel, J., Lauks, I., Chan, P., Babic, D., 1983. The extended gate chemically sensitive field effect transistor as multi-species microprobe. *Sens. Actuators* 4, 291–298.
- van Hal, R., Eijkel, J., Bergveld, P., 1995. A novel description of ISFET sensitivity with the buffer capacity and double-layer capacitance as key parameters. *Sens. Actuators B: Chem.* 24, 201–205.
- van Hal, R., Eijkel, J., Bergveld, P., 1996. A general model to describe the electrostatic potential at electrolyte oxide interfaces. *Adv. Colloid Interface Sci.* 69, 31–62.
- Vanamo, U., 2013. *Solid-State Reference and Ion-Selective Electrodes- Towards Portable Potentiometric Sensing*, Ph.D. thesis, Abo Academi.
- Walsh, K.B., DeRoller, N., Zhu, Y., Koley, G., 2014. Application of ion-sensitive field effect transistors for ion channel screening. *Biosens. Bioelectron.* 54, 448–454.
- Wan, Y., Su, Y., Zhu, X., Liu, G., Fan, C., 2013. Development of electrochemical immunosensors towards point of care diagnostics. *Biosens. Bioelectron.* 47, 1–11.
- Wang, H., Pilon, L., 2011. Accurate simulations of electric double layer capacitance of ultramicroelectrodes. *J. Phys. Chem. C* 115, 16711–16719.
- Wei, F., Lillehoj, P.B., Ho, C.-M., 2010. Dna diagnostics: nanotechnology-enhanced electrochemical detection of nucleic acids. *Pediatr. Res.* 67.
- Welch, D., Shah, S., Ozev, S., Christen, J.B., 2013. Experimental and simulated cycling of isfet electric fields for drift reset. *IEEE Electron Device Lett.* 34, 456–458.
- White, S.P., Dorfman, K.D., Frisbie, C.D., 2015. Label-free dna sensing platform with low-voltage electrolyte-gated transistors. *Anal. Chem.* 87, 1861–1866.
- Xu, G., Abbott, J., Qin, L., Yeung, K.Y.M., Song, Y., Yoon, H., Kong, J., Ham, D., 2014. Electrophoretic and field-effect graphene for all-electrical dna array technology. *Nat. Commun.* 5.
- Xu, G., Abbott, J., Qin, L., Yeung, K.Y.M., Song, Y., Yoon, H., Kong, J., Ham, D., 2015. Electrophoretic and field-effect graphene for all-electrical dna array technology. *Nat. Commun.* 5.
- Zhang, A., Lieber, C.M., 2016. Nano-bioelectronics. *Chem. Rev.* 116, 215–257.
- Zhang, X., Ju, H., Wang, J., 2008. *Electrochemical Sensors, Biosensors and their Biomedical Applications*. Academic Press.
- Zhang, Q., Majumdar, H.S., Kaisti, M., Prabhu, A., Ivaska, A., Österbacka, R., Rahman, A., Levon, K., 2015a. Surface functionalization of ion-sensitive floating-gate field-effect transistors with organic electronics. *IEEE Trans. Electron Devices* 62, 1291–1298.
- Zhang, Q., Prabhu, A., San, A., Al-Sharab, J.F., Levon, K., 2015b. A polyaniline based ultrasensitive potentiometric immunosensor for cardiac troponin complex detection. *Biosens. Bioelectron.* 72, 100–106.
- Zhang, A., Zheng, G., Lieber, C.M., 2016. *Nanowire Field-Effect Transistor Sensors*, Springer International Publishing, Cham, pp. 255–275. [http://dx.doi.org/10.1007/978-3-319-41981-7\\_10](http://dx.doi.org/10.1007/978-3-319-41981-7_10).